Journal of Hazardous Materials 383 (2020) 121130

Contents lists available at ScienceDirect

Journal of Hazardous Materials

journal homepage: www.elsevier.com/locate/jhazmat

Improving laccase activity and stability by HKUST-1 with cofactor via one-pot encapsulation and its application for degradation of bisphenol A

Rongzheng Zhang[a], Lei Wang[a], Juan Han[b], Jiacong Wu[a], Chunmei Li[a], Liang Ni[a], Yun Wang[a,*]

[a] School of Chemistry and Chemical Engineering, Jiangsu University, 301 Xuefu Road, Zhenjiang, 212013, Jiangsu Province, China
[b] School of Food and Biological Engineering, Jiangsu University, 301 Xuefu Road, Zhenjiang, 212013, Jiangsu Province, China

ARTICLE INFO

Editor: Danmeng Shuai

Keywords:
Enzyme immobilization
Laccase
Cofactor
Metal-organic framework
Biomimetic mineralization

ABSTRACT

Enhancing the catalytic activity and stability of enzymes is of great importance in the development of green chemical and cost-effective application, with removal of bisphenol A (BPA) as a prominent example. Engineering immobilization carriers and immobilization methods of enzymes endows great potential to achieve above goal. Until now, these reports have focused on employing the metal-organic frameworks (MOFs) to increase the stability and reusability of enzymes, an enhancement in its catalytic activity has yet to be addressed. This work introduced a biomimetic mineralization process for facile synthesis of laccase@HKUST-1 biocomposite under mild condition. By exploiting the activity of laccase@HKUST-1, we demonstrated, for the first time, that the integration of laccase and HKUST-1 containing cofactor Cu^{2+} ions leaded to 1.5-fold enhancement in the catalytic activity compared with free laccase, which was due to the synergistic enhancement of substrate oxidation. Indeed, the laccase@HKUST-1 biocomposite could function as active biocatalysts under biologically challenging conditions, such as acidic condition, high temperature, organic solvent, and continuous operation. The oxidation of phenols, such as BPA, with laccase@HKUST-1 reached higher catalytic performance than free laccase, and gave 100% degradation efficiency within 4 h. This study provides a feasible method to improve the activity and stability of laccase, which enable completely remove of BPA from the environment.

1. Introduction

Enzymes, as eco-friendly and green biocatalysts, meet the trends of sustainable development and green chemistry as they provide high catalytic efficiency, lower energy requirement, mild reaction condition, and less by-product (Gkaniatsou et al., 2018; Hui et al., 2017; Wang et al., 2019a). As a result, enzymes find numerous applications including pollutant removal, biomass degradation, drug synthesis, and chemical sensing (Wang et al., 2019b; Rong et al., 2018; Han et al., 2018a). Despite many excellent properties in enzymes, they are expensive and fragile, hampering their practical application (Sarma et al., 2017). In general, enzyme immobilized on solid supports to enhance their stability and recovery stimulates their developments and applications.

Recently, numerous carriers, such as synthetic polymers (Limadinata et al., 2015), magnetic nanoparticles (Han et al., 2018b), silica materials (Gao et al., 2017), and metal-organic frameworks (MOFs) (Wang et al., 2017a; Bilal et al., 2018), have been explored for enzyme immobilization. Among these various immobilization supports, metal-organic frameworks (MOFs), a class of porous materials, is the popular one because of its high stability, tunable pore size, large pore volume, high surface area and mild synthesis conditions (Liang et al., 2017; Wang et al., 2019c). These attractive properties have appeared as crucial parameters using as a successful enzyme catalysis carrier, which can facilitate mass transfer while offer superior chemical and thermal protection. For example, recent reports explore the usage of MOFs for encapsulating horseradish peroxidase (HRP), glucose oxidase (GOx) and cytochrome c (Cyt c) via biomimetic mineralization (Zhu et al., 2018; Wang et al., 2017b; Somturk et al., 2015). Notably, the stability and reusability of enzymes encapsulated in MOFs have been enhanced, because of reduced mobility by MOFs and easy recycling via centrifugation. However, to practical applications, immobilized enzymes with enhanced catalytic activity is still a high demand but challenging. Using enzyme active center (metal ions or ligands) as inorganic/organic components constructs the MOFs, which can exhibit enzyme-like activity (Wang et al., 2017a). This strategy offers a promising approach for us to prepare enzyme@MOFs with enhanced catalytic activity.

Consumer products, including powder paints, adhesives and food plastic packing materials have been continuous increase in recent decades (Mtibaa et al., 2018). One of this major environmental

* Corresponding author.
E-mail address: yunwang@ujs.edu.cn (Y. Wang).

https://doi.org/10.1016/j.jhazmat.2019.121130
Received 9 May 2019; Received in revised form 23 August 2019; Accepted 30 August 2019
Available online 31 August 2019
0304-3894/

consequences of these usages is release of a considerable sum of BPA into the environment. Due to toxicity and stable structure of BPA, removing the toxic BPA compounds from the environment in a safe and economic way is an immense need. Laccase, a family of blue multicopper oxidases, contains three types of copper ions namely, type 1 (T1), type 2 (T2), and double type 3 (T3) copper ions. T1 copper is responsible for the oxidation of substrates, and trapped electron. Subsequently, the abstracted electron is transferred from the T1 copper center to the T2 and T3 copper cluster through a Cu-Cys-His pathway. Then the T2 and T3 copper cluster reduce dioxygen to water molecular (Guan et al., 2018; Shao et al., 2019). Thus, laccase can been applied in decomposition of BPA in a safe way (Bilal et al., 2019a). Furthermore, we expect that using copper ions of laccase active center as a structure motif to construct laccase@HKUST-1 biocomposite will enable the enhanced activity and stability of laccase, which could degrade the toxic BPA in cost-effective and safe manner.

In this study, we showed that the encapsulation of laccase in Cu-MOF (HKUST-1) layer could be a valuable strategy for an enhancement in the catalytic activity of laccase. Furthermore, the Cu-MOF not only performed as protective layer against high temperatures, continuous operation and long-term storage but also could enhance the accessibility of active site of laccase due to its flower-like structure and a high exposed surface area. These findings highlight the superior performance of MOFs for enzyme encapsulation to enhance its catalytic activity, stability and reusability compared with other conventional polymers or inorganic carriers.

2. Materials and methods

2.1. Materials

Laccase (from *Trametes versicolor*, powder, 0.5 U·mg^{-1}, EC 1.10.3.2) and 2,2′-azino-bis(3-ethylbenzothiazoline-6-sulfonic acid) (ABTS, 98%) were purchased from Sigma-Aldrich Co. 1,3,5-benzenetricarboxylicacid ($C_9H_6O_6$, 98%) was obtained from Jinan Henghua Sci. & Tec. Co. Ltd. Cupric acetate monohydrate ($Cu(CH_3COO)_2.H_2O$, > 98%) was from Sinopharm (Shanghai, China) Chemical Reagent Co. Ltd. Bisphenol A (BPA: $(CH_3)_2C(C_6H_4OH)_2$, 99%) was purchased from Aladdin. All other chemicals (analytical grade) were from Sinopharm (Shanghai, China) Chemical Reagent Co. Ltd. and used without modification.

2.2. Effect of metal ions and different metal organic frameworks on laccase activity

The effect of metal ions and different metal organic frameworks on laccase activity were detected by several controlled experiments. The method was following, 50 μL of free laccase solution and 300 μL of NaAc-HAc buffer solution (pH 4) were added to the two control experiments. Then 100 μL deionized water and 100 μL ethylenediaminetetraacetic acid (EDTA, 1 M) were added to the two groups of control experiments, respectively. Finally the ABTS was added to measure its activity at 40 °C (Bilal et al., 2019b; Asgher et al., 2017a). In order to investigate the effect of different metal ions on the laccase activity, the activity of free laccase was determined by exposing it to several metal ion solutions such as Cu^{2+}, Zn^{2+}, Li^{+}, Mg^{2+}, K^{+}, Co^{2+}, Mn^{2+}, Ni^{+} and Fe^{2+} (6.25 mM) for 0.5 h at 30 °C. To evaluate which metal-organic framework was beneficial to laccase, two common metal-organic frameworks like HKUST-1 and Zn-MOF were used to immobilize laccase. Subsequently, measuring their activity.

2.3. Enzyme loading

The encapsulation yield of laccase in the HKUST-1 was measured by Pierce™BCA protein assay. The encapsulation yield was defined as the ratio of laccase amount in the laccase@HKUST-1 to the initial amount of laccase. Encapsulation yield was calculated according to the following equation:

$$\text{Encapsulationyield}(\%) = \frac{m - C_1V_1}{m} \times 100\%$$

Where, m (mg) is the mass of laccase initially added to the solution; C_1 (mg/mL) is the laccase concentration of supernatant; V_1 (mL) is the volume of supernatant, respectively.

2.4. Effects of pH and temperature

The effects of pH and temperature on free and immobilized laccase were assessed by measuring the activity in different pH values (pH 3–6.5) and different temperatures (30–70 °C). The method for detecting activity was mentioned above. Taking the optimum activity of laccase@HKUST-1 as 100%. By testing the encapsulation yield, the laccase content in free and immobilized laccase was consistent, and the concentration of laccase in free and immobilized laccase solution was 0.1 mg/ml. In the following experiments, the concentration of laccase was the same as above.

2.5. Thermal stability and pH stability

Thermal stability of laccase and laccase@HKUST- were examined by measuring the residual activity, which were incubated for 1 h at 30–70 °C. The thermal denaturation kinetics of laccase and laccase@HKUST-1 were expressed by a first-order exponential equation. The thermal denaturation constants (k_d) can be calculated according to the Eq. (1). Formula (2) was used to calculate the half-life ($t_{1/2}$) of laccase thermal denaturation. The activation energy (E_d) of laccase thermal denaturation was calculated by the Arrhenius equation (Eq. (3)). The enthalpy (ΔH, kJ·mol^{-1}) for laccase thermal denaturation was calculated according to formula (4).

$$a = a_o \exp(-k_d t) \quad (1)$$

$$t_{1/2} = \ln 2/k_d \quad (2)$$

$$\ln k_d = -E_d/RT + \ln A \quad (3)$$

$$\Delta H = E_d - RT \quad (4)$$

Here, a_0 is the activity of laccase before incubation, a is the residual activity of laccase after incubation, and t (h) is the incubation time. R is a constant 8.3145 J·mol^{-1} K, and T (K) is the absolute temperature.

The pH stability of free and immobilized laccase were examined by incubating free and immobilized laccase in NaAc-HAc solution with different pH values (pH 4–7) for 1 h respectively. Finally, the activity was determined under the optimal conditions. Taking the optimum activity of laccase@HKUST-1 as 100%.

2.6. Calculation of the kinetic parameters

The values of the kinetic values were acquired by non-linear curve fitting of the plot of the reaction rate versus substrate concentrations.

$$\frac{1}{V_0} = \frac{K_m}{V_m} \times \frac{1}{[S]} + \frac{1}{V_m}$$

Where, V_0 is the initial catalytic rate. V_m is the maximum rate conversion. [S] is the initial substrate concentration, and K_m is the Michealis-Menten constant.

2.7. Data analysis

All data in our experiments were derived from three parallel experiments and the average and standard deviation of the replicates were calculated. Student's *t*-test was used to compared whether the difference was significant; $p \leq 0.05$ was adopted as a criterion of significance. The date were analyzed by Microsoft Excel 2010 and Origin

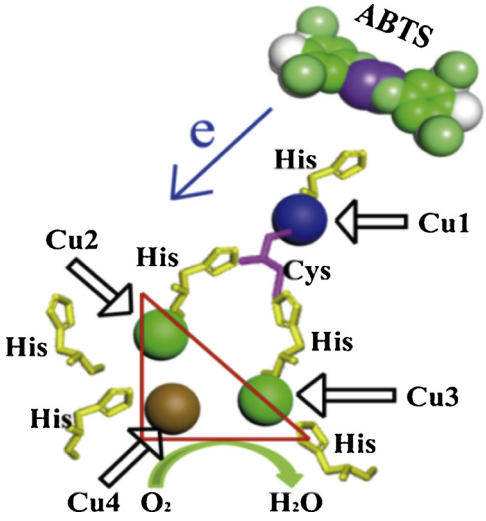

Fig. 1. The electron moves from the T1Cu to the trinuclear cluster through a Cu-Cys-His pathway.

9.0.

3. Results and discussion

3.1. Preparation of laccase@HKUST-1 biocomposite

According to the catalytic mechanism of laccase (Fig. 1), we can see that the catalytic activity of laccase is determined by active center coppers (Granja-Travez et al., 2018). To further demonstrate the effectiveness of HKUST-1 (using laccase active center as a structure motif of MOF) in enhancing the catalytic activity of laccase, laccase activity assay was performed in EDTA solution, solution of various metal ion and different MOFs. As a first step, the free laccase was incubated with EDTA solution. As depicted in Fig. 2a, no dramatically loss in laccase activity occurred when EDTA was added, because the catalytic copper was buried into the active center and more difficult to coordinate with EDTA. Hence, laccase could be not inactivated by the biomineralization, which was due to that organic ligands of MOFs hardly binded catalytic copper and broke down the electron transfer system. Meanwhile, effect of metal ions on catalytic activity of laccase was also evaluated by incubating laccase with the solution of different metal ions. Clearly, only Cu^{2+} ion yielded profoundly positive effect on catalytic activity of laccase with 156 ± 1.3% original activities, as presented in Fig. 2b. Such result was consistent with previously reported results (Sun et al., 2019). An enhancement in catalytic activity observed in incubating laccase with copper ions might be the synergistic effect between laccase and copper ions. On the one hand, copper was the active center of laccase, and the introduction of copper ions had an activation effect on laccase activity. On the other hand, the addition of copper ions accelerated the transfer of electrons between the laccase active centers T1, T2 and T3Cu, thereby increasing the activity. Based on the above results, Cu-MOF (HKUST-1) was adopted as protective layer to construct the laccase@HKUST-1 through biomimetic mineralization. We speculated that synthetic mechanism of laccase@HKUST-1 was that amide groups in the laccase surface coordinated with metal ion, and then act as specific nucleation points to start the biomineralization of MOFs (Scheme 1). As displayed in Fig. 2c, 150 ± 1.3% enhancement of catalytic activity in laccase@HKUST-1 had been achieved compared with the laccase@Zn-MOF (Zn^{2+} ion had a negligible effect on the catalytic activity of laccase). Here, this work highlighted a valuable strategy to enhance the laccase activity by building a bridge of cooperation between laccase and HKUST-1, using the MOF containing cofactor Cu^{2+} as carriers for laccase encapsulation.

The concentrations of cofactor Cu^{2+} ions and organic ligands 1,3,5-benzenetricarboxylicacid (BTC), concentrations of laccase, incubation pH and incubation time were major factors to influence the formation of HKUST-1 shell, which provided the protection of laccase. Therefore, we evaluated the activity and encapsulation yield of laccase during the biomimetic mineralization process of laccase@HKUST-1 in detail to obtain optimum experimental condition. The concentrations of cofactor Cu^{2+} ions and organic ligands BTC had a crucial effect on both activity and encapsulation yield of laccase, as presented in Table S1 and S2. The relative activity and encapsulation yield (defined in the supporting) of laccase kept increasing until 150.1 ± 2.1% and 54 ± 1.1%, respectively, with the enhancement in the concentrations of Cu^{2+} ions up to 87.5 mM and organic ligands BTC up to 25 mM. The continuous increases in the concentrations of Cu^{2+} ions and BTC ligands resulted in a significant reduction in both activity and encapsulation yield of laccase. From further morphology study of the resulting laccase@HKUST-1 biocomposite (Fig. 6), we speculated that microparticles with relatively smooth surfaces led to the smaller chance for the interaction of laccase to the substrate and reduction in activity at high concentrations of Cu^{2+} ions and BTC ligands. Accordingly, high concentrations of Cu^{2+} ions and BTC ligands also generated rapid coordination reaction between Cu^{2+} and BTC, while amine groups in the laccase backbone could not effectively bind with Cu^{2+} ions, resulting in the reduction of encapsulation yield. In order to achieve high activity and encapsulation yield of laccase, 87.5 mM of Cu^{2+} ions and 25 mM of BTC ligands were selected as the optimum concentrations for further evaluation.

Que et al. (2014) reported that laccase isoelectric point (pI) was 4.2, while below and above this value laccase was expected to be positive and negative. To ensure strong electrostatic interactions between the laccase and Cu^{2+} ions for laccase encapsulation, the formation of laccase@HKUST-1 biocomposite was investigated in the pH range of 4.5–7. As illustrated in the Fig. 3a, the laccase@HKUST-1 synthesized with NaAc-HAc solution at pH 6.5 (after the formation of laccase@HKUST-1, the pH of the supernatant was 4.6) had the highest relative activity of 156.7 ± 1.4%. This was because the HKUST-1 protective

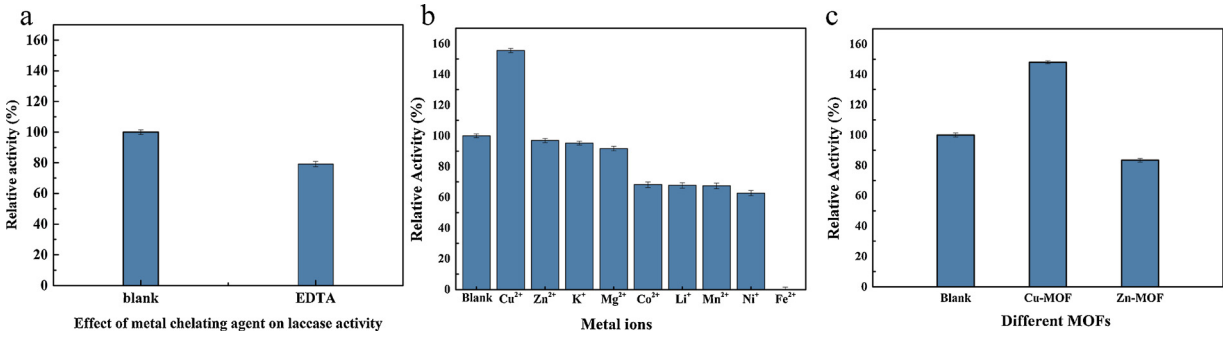

Fig. 2. (a) Effect of center copper ions on the catalytic activity of laccase, (b) Effects of metal ions on laccase activity, (c) Effects of Cu-MOF and Zn-MOF on laccase activity.

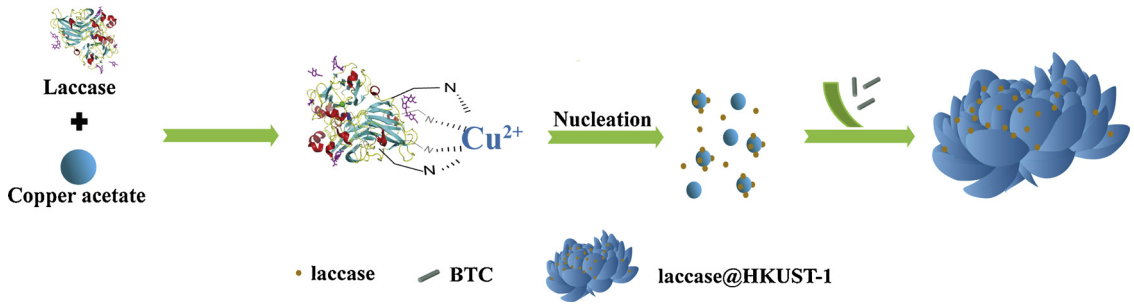

Scheme 1. Schematic illustration of the synthesis of laccase@HKUST-1.

layer was well formed when using acetate buffer solution at the pH 6.5. The result of encapsulation yield of laccase was in accordance with the activity of laccase, which afforded the highest encapsulation yield of laccase, 51.2 ± 1.3%.

The laccase concentration was also another crucial factor for determining the number of nucleation sites, which consequently mediate the formation of HKUST-1 protective layer. As presented in Fig. 3b, we found that 2 mg/mL of laccase was optimal to achieve 153.1 ± 1.6% activity and 56.1 ± 1.4% (147.5 ± 2.1 $mg \cdot g^{-1}$) encapsulation yield. While activity and encapsulation yield began to drop down when adding more than 2 mg/mL of laccase. From results, 2 mg/mL of laccase was determined to properly form the laccase@HKUST-1.

Incubation time played an important role in the activity and encapsulation yield of laccase. Fig. 3c showed incubation time of 8 h appeared to be more effective for encapsulating laccase compared to the lower and higher incubation time of 8 h, giving 153 ± 2.1% and 53.4 ± 1.8% activity and encapsulation yield, respectively. Considering the activity and encapsulation yield, 8 h was chosen as an appropriate incubation time for laccase encapsulation.

3.2. Characterization of laccase@HKUST-1 biocomposite

Successful encapsulation of laccase by HKUST-1 shell was ascertained by FT-IR spectrum. Firstly, the biomineralized laccase@HKUST-1 was washed with water to ensure the removal of surface bound laccase, and then characterized by FT-IR spectrum. As displayed in Fig. 4a, The FT-IR of laccase@HKUST-1 was similar to HKUST-1, with the exception of the peaks at 1657.43 cm^{-1} belong to C═O stretching vibration due to the presence of laccase. Other characteristic peaks of laccase were also present in the FT-IR spectrum. For example, the peaks appeared at 1029.93 and 1544.56 cm^{-1}, ascribing to a band of enzyme and combination between N—H bending vibration and C–N stretching vibration of the amide bond. As expected, the above peaks were still emerged in the FT-IR spectrum of laccase@HKUST-1 biocomposite. The results were consistent with A. Samui et al. (Samui and Sahu, 2018), signifying the successful fabrication of laccase@HKUST-1. Subsequently, we studied the laccase@HKUST-1 by energy dispersive X-ray spectroscopy (EDS). The presence of N element provided the evidence that the laccase had been encapsulated in HKUST-1.

The quantity of laccase within lacacse@HKUST-1 was determined to examine by TGA curves. For laccase@HKUST-1, The TGA curve showed two obvious weight loss steps (Fig. 4b). The first weight loss below 125 °C was probably as a result of the evaporation of adsorbed and bound water. A deeper weight drop from 125 to 320 °C might be attributed to decomposition of laccase. The loss quantity of laccase was calculated to be approximate 12%. The weight percentages of laccase in HKUST-1 was consistent with the encapsulation yield of laccase determined by Pierce™ BCA protein measurement (14.75%).

Further morphology and crystallinity of laccase@HKUST-1 biocomposite was characterized by scanning electron microscopy (SEM), transmission electron microscope (TEM) and X-ray diffraction (XRD). The results of morphology of HKUST-1 and laccase@HKUST-1 were shown in Fig. 5. HKUST-1 were regular acicular structures (Fig. 5a), exhibiting average sizes of 1 μm. Different from the HKUST-1, laccase@HKUST-1 (Fig. 5b) formed microflower whose broad particle size distribution range from 1 to 1.5 μm. These different morphologies of HKUST-1 and laccase@HKUST-1 biocomposite were attributed to aggregative growth kinetics mediated by laccase, which made the formation of microflower structure become possible. Laccase@HKUST-1 was further investigated by transmission electron microscope (TEM). As displayed in Fig. 5c, it exhibited the same morphology with the SEM images of laccase@HKUST-1. From the XRD patterns of HKUST-1 and laccase@HKUST-1 (Fig. 5d), we could clearly see that there was no visible difference with regard to the crystalline structure between the pure HKUST-1 and laccase@HKUST-1 biocomposite because the positions of all diffraction peaks matched well. The results showed that the structural integrity and crystalline form of HKUST-1 could be preserved in the presence of laccase.

For the morphology study of laccase@HKUST-1 biocomposite, the synthesis of laccase@HKUST-1 biocomposite was conducted at various BTC and Cu^{2+} concentrations. As presented in Fig. 6, there was a great variation in morphology of the resulting laccase@HKUST-1 biocomposite by means of regulating the concentrations of BTC ligand and Cu^{2+} ion. Highly elaborate microflowers were formed at lower

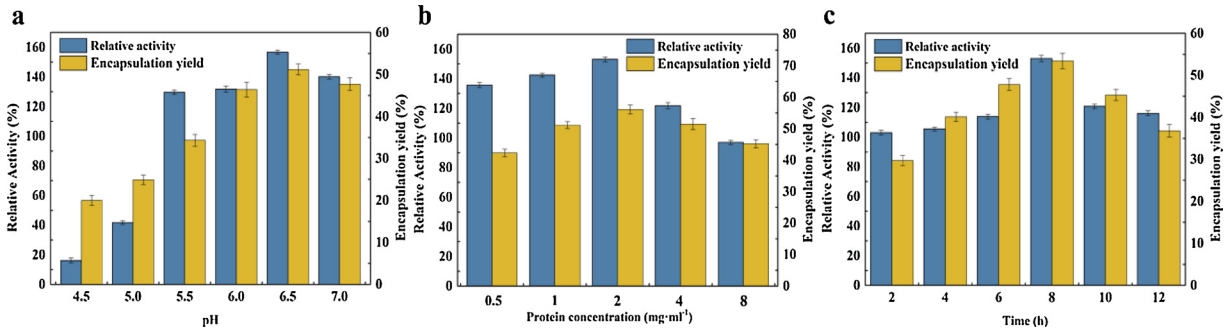

Fig. 3. (a) Effect of incubating pH, (b) concentration of laccase and (c) incubating time on relative activity and encapsulation capacity of laccase@HKUST-1 biocomposite.

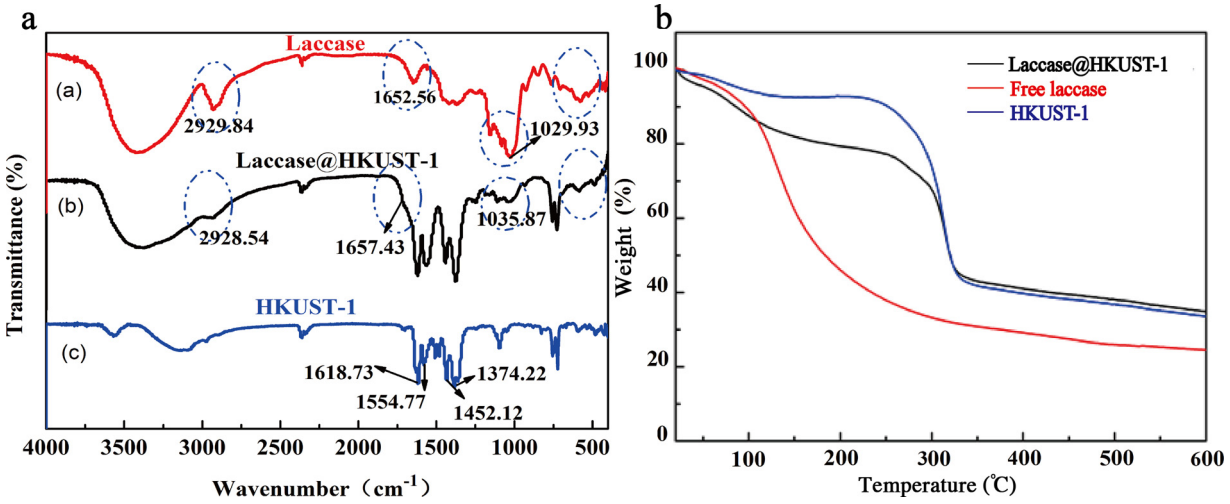

Fig. 4. (a) FT-IR spectra of free laccase, laccase@HKUST-1 and HKUST-1, (b) TGA curves of laccase@HKUST-1, free laccase and HKUST-1.

concentrations of organic BTC ligand and Cu^{2+} ion. Upon an increase in the concentrations of organic BTC ligand and Cu^{2+} ion to 62.5 mM and 100 mM, respectively, nanoparticles would be generated instead of microflowers. These microflowers with insufficient blooming morphology were observed when the concentrations of organic BTC ligand and Cu^{2+} ion were lower than 62.5 mM and 100 mM, respectively. This microflower structure of laccase@HKUST-1 afforded a high exposed surface area and enabled a greater chance for effective interaction with substrate (Cui et al., 2017). All these observations suggested the concentrations of BTC ligand and Cu^{2+} ion responded to the morphology of laccase@HKUST-1 biocomposite, and further affects the activity of encapsulated laccase.

3.3. Optimal pH and temperature

It is well known that the catalytic activity of laccase and laccase@HKUST-1 is dependent on reaction conditions. To obtain the maximum activity of laccase and laccase@HKUST-1, the effects of reaction pH and temperature on catalytic activity of free laccase and laccase@HKUST-1 were evaluated. As shown in Fig. 7a, the maximum activity for laccase@HKUST-1 was achieved at pH 4, which was identical with that of laccase. When the pH was above or below 4, the catalytic activity of both laccase@HKUST-1 and laccase exhibited a downward trend. Interestingly, laccase@HKUST-1 expressed a much higher activity than laccase under identical pH conditions. For example, laccase@HKUST-1 maintained 78.7 ± 0.9% and 75.3 ± 0.8% of its maximum activity at pH 3.0 and 5.5, respectively. However, laccase retain only 45.3 ± 1.2% and 42.2 ± 0.9% activity, correspondingly ($p \leq 0.05$).

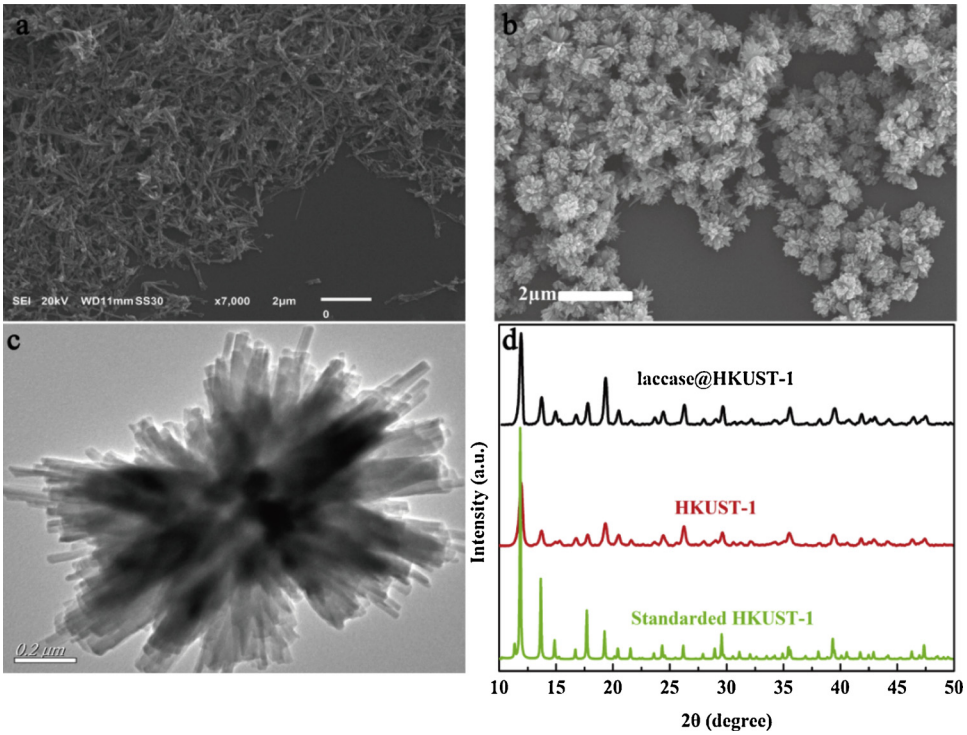

Fig. 5. (a) SEM images of the pure HKUST-1 and (b) laccase@HKUST-1 biocomposite. (c) TEM images showing laccase@HKUST-1 composites. (d) XRD patterns of pure laccase@HKUST-1 biocomposite, HKUST-1 and standard HKUST-1.

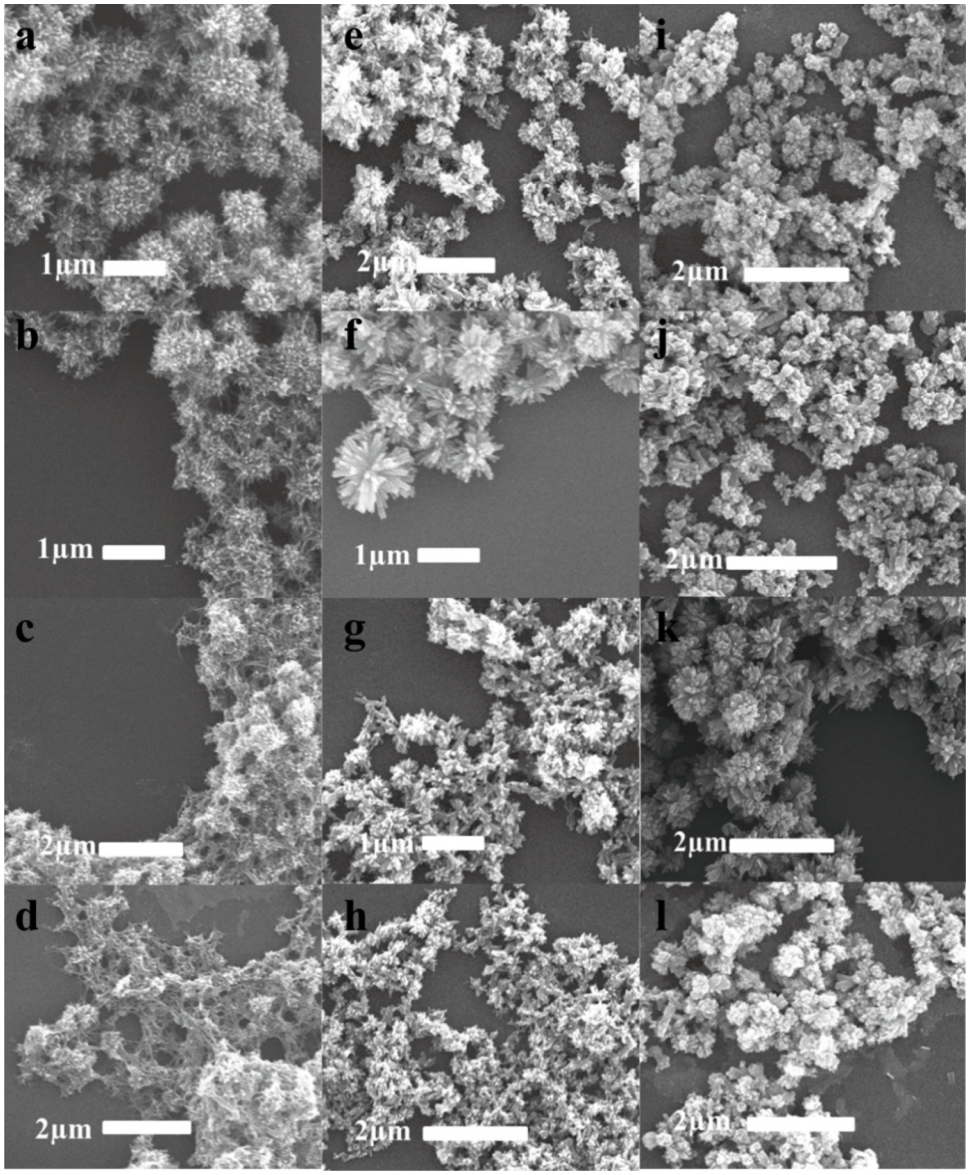

Fig. 6. SEM images showing laccase@HKUST-1 composites obtained using various copper ions concentrations: (a, e, i) 62.5 mM, (b, f, j) 75 mM, (c, g, k) 87.5 mM, (d, h, l) 100 mM and BTC concentrations: (a–d) 6.25 mM, (c–h) 12.5 mM, (i–l) 25 mM.

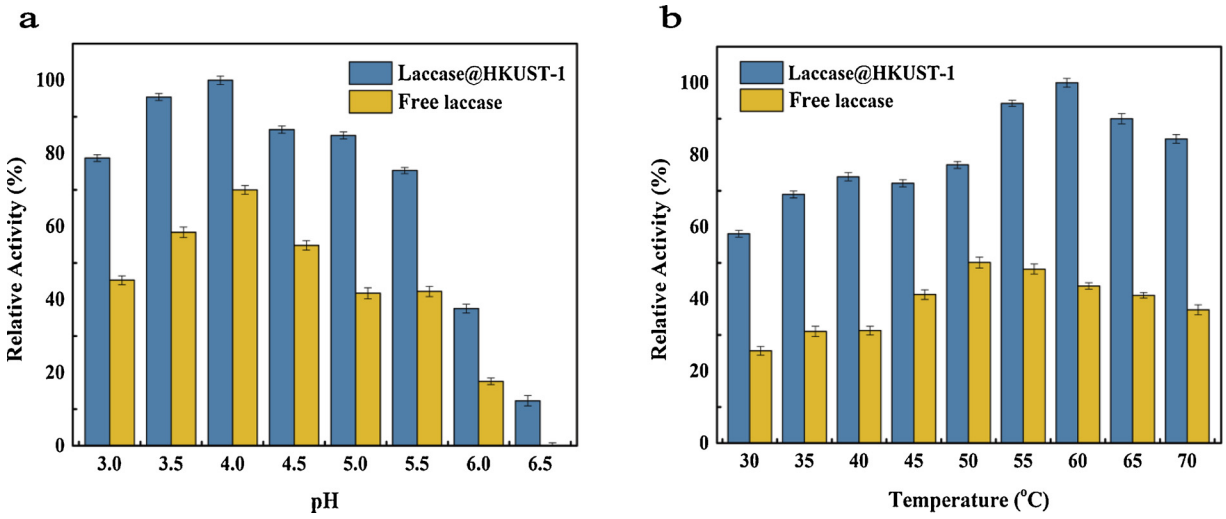

Fig. 7. (a) Effects of reaction pH and (b) temperature on catalytic activity of free laccase and laccase@HKUST-1.

Table 1
Kinetic parameters of free laccase and laccase@HKUST-1.

Kinetic parameter	K_m(g·L^{-1})	K_{cat}(min^{-1})	V_m(g·L^{-1}·min^{-1})	K_{cat}/K_m
Free laccase	0.0251	0.853	0.1706	33.984
Laccase@HKUST-1	0.0189	2.3175	0.4635	122.619

These higher catalytic activities for laccase@HKUST-1 arose from the suitable buffering function of HKUST-1 (Nguyen et al., 2016) and positive effects of cofactor Cu^{2+} ion on the enzymatic activity (Khambhaty et al., 2015; Rong et al., 2017).

The temperature-dependent activity of the pristine laccase and laccase@HKUST-1 biocomposite was also conducted in the temperature range from 30 to 70 °C. The results indicated that the optimum temperature for laccase was 50 °C, and when the temperature above 50 °C, the catalytic activity of pristine laccase significantly decreased. Compared with laccase, laccase@HKUST-1 had the highest catalytic activity at the temperature as high as 60 °C ($p \leq 0.05$), which proved that the protective effect of the HKUST-1 coating that limited the flexibility of laccase, subsequently preventing laccase from heat-induced denaturation (Liang et al., 2019; Mohammad et al., 2019; Asgher et al., 2017b).

To better understand the effect of HKUST-1 to the substrate binding efficiency of laccase and catalytic efficiency (Shown Table 1 and Fig. S2), the kinetic parameters and K_{cat}/K_m of both laccase and laccase@HKUST-1 were studied in this work. The K_m for laccase was 0.0251 g·L^{-1}. A decrease in K_m for laccase@HKUST-1 was presented, suggesting that laccase@HKUST-1 had stronger affinity to the substrate in comparison with free laccase. After the encapsulation of laccase by HKUST-1, HKUST-1 created a microenvironment which made the encapsulated laccase effectively contact with substrate. In terms of the catalytic efficiency, K_{cat}/K_m for laccase@HKUST-1 improved by nearly 4 times of that for the laccase. The result indicated the enhance of laccase activity to convert substrate into product, which might be related to higher surface area of the unique flower-like structure and the presence of cofactor Cu^{2+} ions. The stronger affinity of laccase@HKUST-1 to substrate, together with the improved activity, confirmed the favorable effect of HKUST-1.

3.4. Stability and reusability of laccase@HKUST-1 biocomposite

Exposure of the enzyme to harsh environments (for example, acidic conditions, elevated temperatures, and organic solvents) typically results in loss of activity. The better stability of encapsulated enzymes was an essential criterion for industrial applications. In order to obtain an insight into the efficiency of HKUST-1 shell to increase the acidic stability of activity, we tested the activity of laccase and laccase@HKUST-1 after incubation for 1 h under different acidic conditions. As demonstrated in Fig. 8a, under acidic conditions, the HKUST-1 made laccase more active than free laccase ($p \leq 0.05$). This is because the acidic material HKUST-1 has a protective effect on laccase.

Temperature induced denaturation of laccase was also a major concern when considering the wide range of industrial applications of enzymes. As shown in Fig. 8b, the laccase and laccase@HKUST-1 revealed their highest thermo-stability at 30 °C and 35 °C, respectively. Moreover, the activity of laccase@HKUST-1 was higher than that of laccase at each temperature. F. (Lassouane et al. (2019)) reported that the immobilization of laccase by glutaraldehyde cross-linking into Ca-alginate beads exhibited 25% activity at 60 °C. Whereas, in our study, at the same temperature, the laccase@HKUST-1 could maintain more than 42.8 ± 1.2% activity ($p \leq 0.05$). By comparing the residual activity between the biomimetic mineralization method and the cross-linking method, we could find that the thermo-stability by biomimetic mineralization approach was excellent and much better than that by cross-linking method. This phenomenon should be accounted for the following reasons. In solution, high temperature caused the enzyme to aggregate and form a disordered structure. For laccase@HKUST-1, the HKUST-1 coating had a rigid structure, which can limit the flexibility of the enzyme and prevent its folding at high temperatures (Zhao et al., 2011). Thus, the thermal stability of laccase@HKUST-1 increased. The enhancement in the thermal stability of laccase@HKUST-1 was also supported by the stability parameters and change in enthalpy (ΔH°) of the laccase and laccase@HKUST-1, which were present in Tables 2 and 3. Compared thermal denaturation constants (k_d) and half-lives ($t_{1/2}$) of laccase@HKUST-1 with that of laccase at the same temperature, laccase@HKUST-1 exhibited a lower k_d value than the free enzyme and its $t_{1/2}$ value was higher than the free enzyme. This result indicated that laccase@HKUST-1 had a better stability against high temperature. The reason could be seen from the changes in ΔH value. The ΔH value of free and encapsulated laccase began to decrease with the increase in the temperature, which proved that the less energy was needed for inactivation of laccase at higher temperature. In addition, at the same temperature, the ΔH values of laccase@HKUST-1 were higher than that of free enzyme, indicating that the laccase@HKUST-1 required higher energy to inactivate than free laccase. Conversely, laccase@HKUST-1 was more thermally than laccase.

To examine the tolerance of polar solvents including methanol (MeOH), ethanol (EtOH), dichloromethane (DCM), dimethyl sulfoxide (DMSO), methyl cyanide (MeCN) and Dimethyl Formamide (DMF). The laccase@HKUST-1 and laccase were incubated in these polar solvents (30% (v/v) polar solvent and deionized water) for 1 h (see Figure S3). The laccase@HKUST-1 almost did not deactivate under all above polar solvents, while an approximately 40 ± 1.2% and 75 ± 1.5% drop in activity of native laccase was observed in MeCN and MeOH, respectively ($p \leq 0.05$). The possible reason was that the organic solvent deprives the "essential water" of the laccase surface and also caused a change in the laccase conformation. But the HKUST-1 protected the laccase activity by preventing essential water from being deprived, so the tolerance of laccase@HKUST-1 to organic solvent was higher than laccase.

Long-term storage stability of laccase@HKUST-1, stored at 4 °C, was checked by assessing its residual activity (Fig. 8c). As expected, laccase@HKUST-1 retained nearly 70 ± 1.6% of initial viability after 30 days, while free laccase retained only 10 ± 1.1% of enzyme activity after 30 days ($p \leq 0.05$). From the result we could know that the excellent durability of the laccase@HKUST-1 revealed great potential in industrial application.

In order to evaluate the reusability of the prepared biocatalyst, laccase@HKUST-1 was separated from the substrate solution after each catalytic reaction, thoroughly washed with deionized water, and finally immersed in fresh substrate for recycling. After being recycled 10 cycles, the residual activity still retained 78.9 ± 1.5% of the initial activity (The reaction was repeated for 10 times and set the initial activity as 100% activity.) (Fig. 8d, $p \leq 0.05$). The reason for this phenomenon is that their size is too small, so that part of the laccase@HKUST-1 are lost during the recovery process. On the other hand, part of laccase are folded or denatured during the reaction with the substrate, resulting in inactivation.

A. Samui et al. (Samui and Sahu, 2018) investigated the immobilization of laccase on the surface of NH_2-MIL-53 (Al). Their results showed that the immobilized laccase maintained about 63% of its initial activity after 10 cycles of usage. Compared with the results of previous studies by Arpita Samui et al., the retention of highly active laccase@HKUST-1 at the same number of cycles had a distinctive advantage. The recyclability of laccase@HKUST-1 demonstrates that laccase was properly encapsulated in the HKUST-1 to prevent denaturation and leaching. All of the above results indicated that the protection of laccase by HKUST-1 could greatly improve the stability of laccase, and the feasibility of laccase extended application range in industry.

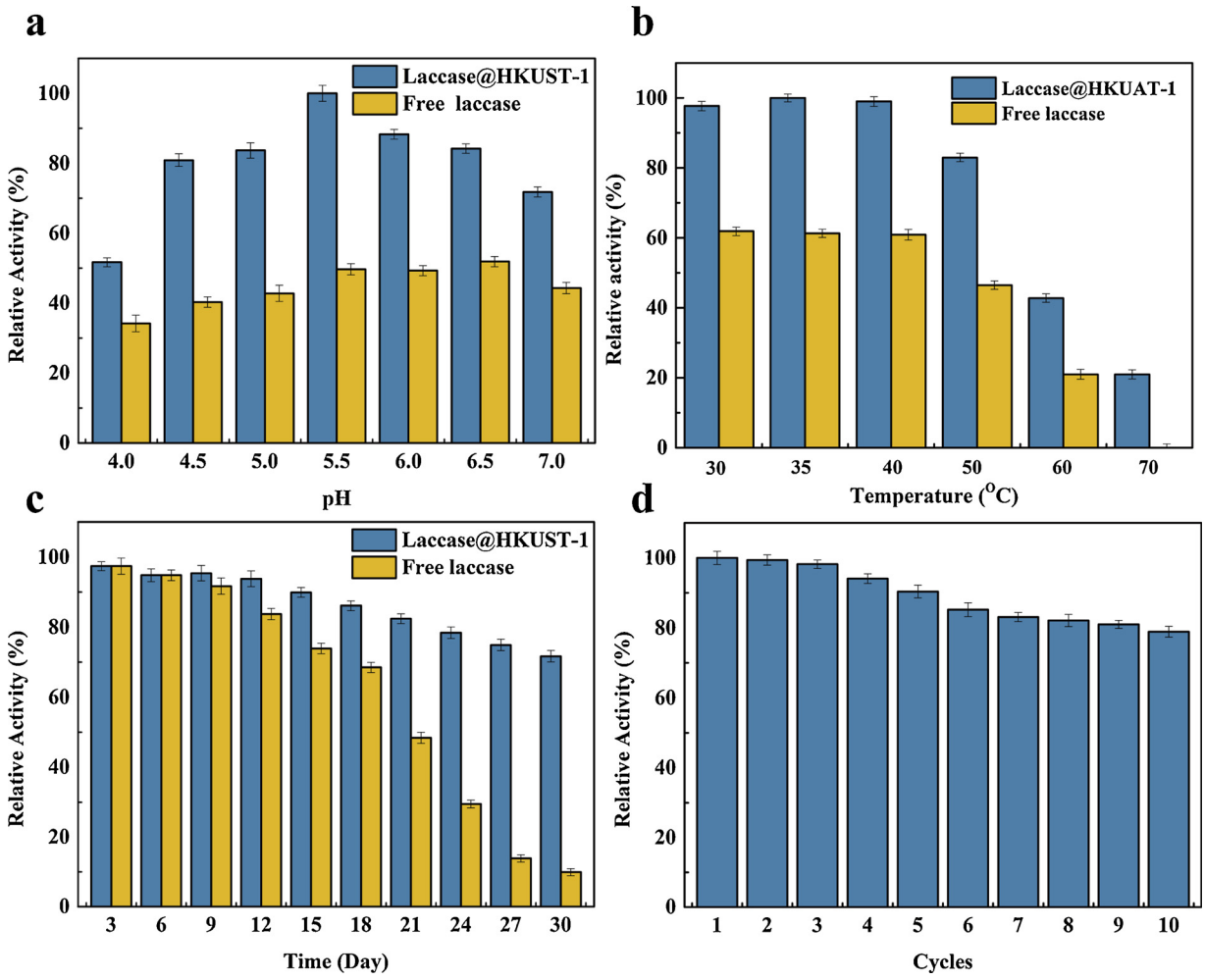

Fig. 8. (a) Incubation pH stability of laccase and laccase@HKUST-1. (b) Incubation temperature stability of laccase and laccase@HKUST-1. (c) Storage stability of laccase and laccase@HKUST-1. (d) Cycle stability of laccase@HKUST-1.

Table 2
Thermal denaturation kinetic parameters and half-life of free laccase and laccase@HKUST-1.

	k_d (h^{-1})		$t_{1/2}$ (h)	
temperature (°C)	free laccase	laccase@HKUST-1	free laccase	laccase@HKUST-1
30	0.0984	0.0403	7.04	17.20
35	0.1232	0.0167	5.63	41.51
40	0.1288	0.0235	5.38	29.50
50	0.3839	0.2025	1.80	3.42
60	1.1920	0.8610	0.58	0.81
70	6.4200	3.1577	0.11	0.22

The error is ± 1.7%. Each data was repeated three times.

Table 3
Change in enthalpy (ΔH) for the thermal denaturation of free laccase and laccase@HKUST-1.

	ΔH (kJ•mol^{-1})	
temperature (°C)	free laccase	laccase@HKUST-1
30	86.8770	109.8832
35	86.8354	109.8416
40	86.7938	109.8000
50	86.7107	109.7169
60	86.6275	109.6337
70	86.5444	109.5506

The error is ± 1.7%. Each data was repeated three times.

3.5. BPA degradation by free laccase and immobilized laccase

The degradation efficiency of free laccase for BPA at pH 4.5 and 40 °C during 8 h was compared with that adding ABTS to the reaction system. Laccase/ABTS system showed 50% higher degradation efficiency for BPA than free laccase (Fig. S8). The results showed that the degradation efficiency of BPA with ABTS was significantly higher than that without ABTS. The possible reason was that laccase mediator ABTS could improve the ability of electron transfer during the degradation reaction (Mir-Tutusaus et al., 2014; Xie et al., 2015). Considering higher degradation efficiency for BPA, ABTS was added to the laccase@HKUST-1 system in this study.

The optimal reaction conditions for degrading BPA were demonstrated by conducting the degradation of BPA in different BPA concentrations, pH, temperatures and reaction times. Within 12 h, laccase@HKUST-1 afforded 98% degradation efficiency at the high concentrations of BPA (higher than 200 mg L^{-1}) (Fig. S4). Whereas, a significant drop in the degradation efficiency by free laccase was observed at 200 mg L^{-1} of BPA. Thus, the concentration of 200 mg L^{-1} for BPA was chosen as the optimum substrate concentration. In the pH range from 4.5 to 7, the optimum pH for degrading BPA by laccase@HKUST-1 at 12 h was 6.5 and free enzyme was 6.0, where the degradation of BPA reached about 99% and 69%, respectively (Fig. S5).

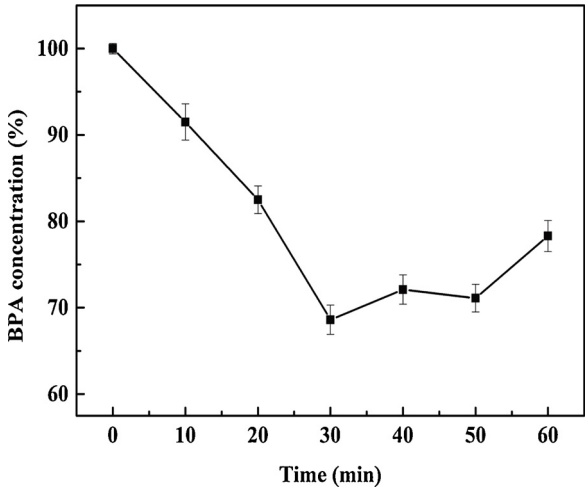

Fig. 9. Adsorption experiment of laccase@HKUST-1 for BPA.

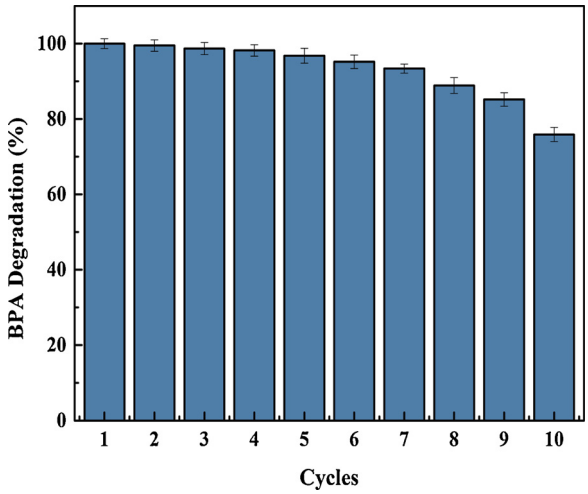

Fig. 10. The degradation cycle of BPA with laccase@HKUST-1 biocomposite.

To provide the excellent degradation performance, the following experiments were conducted at pH of 6.5. By increasing the temperature to 40 °C, laccase and laccase@HKUST-1 improved the degradation efficiency of BPA to 65% and 98.2%, respectively (Fig. S6). Furthermore, an increase of temperature resulted in a decrease in degradation efficiency of BPA for laccase. At a higher temperature, laccase@HKUST-1 did not show a decrease in degradation efficiency. The time course for degrading BPA with laccase@HKUST-1 at 40 °C and pH of 6.5 was then examined (Fig. S7). Laccase@HKUST-1 reached full degradation of BPA at 4 h, while 35.5% degradation efficiency was achieved for laccase at 4 h. The laccase@HKUST-1 gave a lower degradation time than laccase, due to the highly catalytic activity and enhancement of stability.

The adsorption of laccase@HKUST-1 was also tested with the thermal inactivated laccase. Fig. 9 showed that around 25% removal for BPA was achieved via adsorption during 1 h's treatment. In this experiment, the removal for BPA after 4 h by free laccase was 35.5%. In contrast, with the exception of adsorption, the removal for BPA after 4 h by laccase@HKUST-1 was 74.2%. Therefore, the removal for BPA by laccase@HKUST-1 is still higher than that of laccase. In other words, the activity of laccase@HKUST-1 is higher than laccase.

The reusability of laccase@HKUST-1 was carried out in degradation of BPA at 40 °C for 4 h. In each cycle of degradation, laccase@HKUST-1 could be easily recovered through centrifugation, followed by washing with water. Then the obtained laccase@HKUST-1 was used to start the new cycle of degradation of BPA. As evident from the Fig. 8d, after 8 cycles of degradation, a loss of only 12% of its original degradation efficiency was displayed by the laccase@HKUST-1. Further studies showed the laccase@HKUST-1 still maintained 75.9% of its original degradation efficiency after 10 cycles (Fig. 10). This good recycling performance of laccase@HKUST-1 was very beneficial for reducing the cost of BPA degradation.

4. Conclusions

In conclusion, we first investigated the synthesis of laccase@HKUST-1 by using HKUST-1 to encapsulate laccase. HKUST-1 was an acidic material, which allowed laccase to react at optimal pH and protected it in extreme environments. In addition, copper was a cofactor of laccase, and the copper in laccase@HKUST-1 could also increase the activity of laccase. In this experiment, laccase@HKUST-1 demonstrated better pH stability, thermal stability and storage stability compared to free laccase, and had good practical potential in the treatment of industrial BPA wastewater. Accordingly, the method of employing HKUST-1 as a protective layer to protect the laccase against industrial environment provides the possibility to further develop biocomposite for industrial applications.

Acknowledgement

This work was supported by the National Natural Science Foundation of China (Nos. 21676124 and 21878131)

Appendix A. Supplementary data

Supplementary material related to this article can be found, in the online version, at doi:https://doi.org/10.1016/j.jhazmat.2019.121130.

References

Asgher, M., Noreen, S., Bilal, M., 2017a. Enhancement of catalytic, reusability, and long-term stability features of *Trametes versicolor* IBL-04 laccase immobilized on different polymers. Int. J. Biol. Macromol. 95, 54–62.

Asgher, M., Noreen, S., Bilal, M., 2017b. Enhancing catalytic functionality of *Trametes versicolor* IBL-04 laccase by immobilization on chitosan microspheres. Chem. Eng. Res. Des. 119, 1–11.

Bilal, M., Adeel, M., Rasheed, T., Iqbal, H.M.N., 2018. Multifunctional metal–organic frameworks-based biocatalytic platforms: recent developments and future prospects. J. Mater. Res. Technol. 533, 13.

Bilal, M., Iqbal, H.M.N., Barcelo, D., 2019a. Mitigation of bisphenol A using an array of laccase-based robust bio-catalytic cues. Sci. Total Environ. 689, 160–177.

Bilal, M., Jinga, Z., Zhaoa, Y.P., Iqbal, H.M.N., 2019b. Immobilization of fungal laccase on glutaraldehyde cross-linked chitosan beads and its bio-catalytic potential to degrade bisphenol A. Biocatal. Agric. Biotechnol. 19, 101174.

Cui, J.D., Feng, X.Y., Lin, T., Tan, Z.L., Zhong, C., Jia, S.R., 2017. Mesoporous metal-organic framework with well-defined cruciate flower-like morphology for enzyme immobilization. ACS Appl. Mater. Interfaces 9, 10587–10594.

Gao, J., Wang, Y., Du, Y.J., Zhou, L.Y., He, Y., Ma, L., Yin, L.Y., Kong, W.X., Jiang, Y.J., 2017. Construction of biocatalytic colloidosome using lipase-containing dendritic mesoporous silica nanospheres for enhanced enzyme catalysis. Chem. Eng. J. 317, 175–186.

Gkaniatsou, E., Sicard, C., Ricoux, R., Benahmed, L., Bourdreux, F., Zhang, Q., Serre, C., Mahy, J.P., Steunou, N., 2018. Enzyme encapsulation in mesoporous metal–organic frameworks for selective biodegradation of harmful dye molecules. Angew. Chem. Int. Ed. 57, 16141–16146.

Granja-Travez, R.S., Wilkinson, R.C., Persinoti, G.F., Fulop, F.M.V., Bugg, T.D.H., 2018. Structural and functional characterisation of multi-copper oxidase CueO from lignin-degrading bacterium *Ochrobactrum sp* reveal its activity towards lignin model compounds and lignosulfonate. FEBS J. 258, 1684–1700.

Guan, Z.B., Luo, Q., Wang, H.R., Chen, Y., Liao, X.R., 2018. Bacterial laccases: promising biological green tools for industrial applications. Cell. Mol. Life Sci. 75, 3569–3592.

Han, J., Wan, J., Wang, Y., Wang, L., Li, C.M., Mao, Y.L., Ni, L., 2018a. Recyclable soluble-insoluble upper critical solution temperature-type poly(methacrylamide-co-acrylic acid)-cellulase biocatalyst for hydrolysis of cellulose into glucose. ACS Sustain. Chem. Eng. 6, 7779–7788.

Han, J., Wang, L., Wang, Y., Dong, J., Tang, X., Ni, L., Wang, L., 2018b. Preparation and characterization of Fe_3O_4-NH_2@4-arm-PEG-NH_2, a novel magnetic four-arm polymer-nanoparticle composite for cellulase immobilization. Biochem. Eng. J. 130, 90–98.

Hui, L., Jingwei, H., Linlin, D., Chao, J., Yatao, Z., Vicki, C., 2017. Graphene oxide-enzyme hybrid nanoflowers for efficient water soluble dye removal. J. Hazard. Mater.

338, 93–101.
Khambhaty, Y., Ananth, S., Sreeram, K.J., Rao, J.R., Nair, B.U., 2015. Dual utility of a novel, copper enhanced laccase from *Trichoderma* aureoviridae. Int. J. Biol. Macromol. 81, 69–75.
Lassouane, F., Ait-Amar, H., Amrani, S., Rodriguez-Couto, S., 2019. A promising laccase immobilization approach for bisphenol A removal from aqueous solutions. Bioresour. Technol. 271, 360–367.
Liang, K., Richardson, J.J., Doonan, C.J., Mulet, X., Ju, Y., Cui, J.W., Caruso, F., Falcaro, P., 2017. An enzyme-coated metal-organic framework shell for synthetically adaptive cell survival. Angew. Chem. Int. Ed. 56, 8510–8515.
Liang, W.B., Xu, H.S., Carraro, F., Maddigan, N.K., Li, Q.W., Bell, S.G., Huang, D.M., Tarzia, A., Solomon, M.B., Amenitsch, H., Vaccari, L., Sumby, C.J., Falcaro, P., Doonan, C.J., 2019. Enhanced activity of enzymes encapsulated in hydrophilic metal-organic frameworks. J. Am. Chem. Soc. 141, 2348–2355.
Limadinata, P.A., Li, A.T., Li, Z., 2015. Temperature-responsive nanobiocatalysts with an upper critical solution temperature for high performance biotransformation and easy catalyst recycling: efficient hydrolysis of cellulose to glucose. Green Chem. 17, 1194–1203.
Mir-Tutusaus, J.A., Masis-Mora, M., Corcellas, C., Eljarrat, E., Barcelo, D., Sarra, M., Caminal, G., Vicent, T., Rodriguez-Rodriguez, C.E., 2014. Degradation of selected agrochemicals by the white rot fungus Trametes versicolor. Sci. Total Environ. 500, 235–242.
Mohammad, M., Razmjou, A., Liang, K., Asadnia, M., Chen, V., 2019. Metal-organic-framework-based enzymatic microfluidic biosensor via surface patterning and biomineralization. ACS Appl. Mater. Interfaces 11, 1807–1820.
Mtibaa, R., Olicon-Hernandez, D.R., Pozo, C., Nasri, M., Mechichi, T., Gonzalez, J., Aranda, E., 2018. Degradation of bisphenol A and acute toxicity reduction by different thermo-tolerant ascomycete strains isolated from arid soils. Ecotoxicol. Environ. Saf. 156, 87–96.
Nguyen, T.A., Fu, C.C., Juang, R.S., 2016. Effective removal of sulfur dyes from water by biosorption and subsequent immobilized laccase degradation on crosslinked chitosan beads. Chem. Eng. J. 304, 313–324.
Que, Y.X., Sun, S.J., Xu, L.P., Zhang, Y.Y., Zhu, H., 2014. High-level coproduction, purification and characterisation of laccase and exopolysaccharides by Coriolus versicolor. Food Chem. 159, 208–213.
Rong, J.H., Han, J., Zhou, Y., Wang, L., Li, C.M., Wang, Y., 2018. Process integration of production, purification, and immobilization of β-glucosidase by constructing glulinker-ELP-GB system. Ind. Eng. Chem. Res. 57, 15620–15631.
Rong, J., Zhang, T., Qiu, F.X., Zhu, Y., 2017. Preparation of efficient, stable, and reusable laccase–$Cu_3(PO_4)_2$ hybrid microspheres based on copper foil for decoloration of congo red. ACS Sustain. Chem. Eng. 5, 4468–4477.
Samui, A., Sahu, S.K., 2018. One-pot synthesis of microporous nanoscale metal organic frameworks conjugated with laccase as a promising biocatalyst. New J. Chem. 42, 4192–4200.
Sarma, R., Islam, S., Miller, A.-F., Bhattacharyya, D., 2017. Layer-by-layer-assembled laccase enzyme on stimuli-responsive membranes for chloro-organics degradation. ACS Appl. Mater. Interfaces 9, 14858–14867.
Shao, B.B., Liu, Z.F., Zeng, G.M., Liu, Y., Yang, X., Zhou, C.Y., Chen, M., Liu, Y.J., Yan, Y.L.M., 2019. Immobilization of laccase on hollow mesoporous carbon nanospheres: noteworthy immobilization, excellent stability and efficacious for antibiotic contaminants removal. J. Hazard. Mater. 362, 318–326.
Somturk, B., Hancer, M., Ismail, O.B., Ozdemir, N., 2015. Synthesis of copper ion incorporated horseradish peroxidase-based hybrid nanoflowers for enhanced catalytic activity and stability. Dalton Trans. 44, 13845–113852.
Sun, K., Li, S.Y., Yu, J.L., Gong, R., Si, Y.B., Liu, X.H., Chu, G., 2019. Cu^{2+}-assisted laccase from *Trametes versicolor* enhanced self-polyreaction of triclosan. Chemosphere 225, 745–754.
Wang, L., Li, W., Liu, Y., Zhi, W., Han, J., Wang, Y., Ni, L., 2019a. Green separation of bromelain in food sample with high retention of enzyme activity using recyclable aqueous two-phase system containing a new synthesized thermo-responsive copolymer and salt. Food Chem. 282, 48–57.
Wang, Q.Q., Zhang, X.P., Huang, L., Zhang, Zh.Q., Dong, S.J., 2017a. GOx@ZIF-8(NiPd) nanoflower: an artificial enzyme system for tandem catalysis. Angew. Chem.-Int. Edit. 56, 16082–16085.
Wang, L., Zhi, W.J., Lian, D.S., Wang, Y., Han, J., Wang, Y., 2019b. HRP@ZIF-8/DNA hybrids: functionality integration of ZIF-8 via biomineralization and surface absorption. ACS Sustain. Chem. Eng. https://doi.org/10.1021/acssuschemeng.9b02348.
Wang, Q.Q., Zhang, X.P., Huang, L., Zhang, Z.Q., Dong, S.J., 2017b. GOx@ZIF-8(NiPd) Nanoflower: An artificial enzyme system for tandem catalysis. Angew. Chem. Int. Ed. 56, 16082–16085.
Wang, L., Zhi, W.J., Wan, J., Han, J., Li, C.M., Wang, Y., 2019c. Recyclable β-glucosidase by one-pot encapsulation with Cu-MOFs for enhanced hydrolysis of cellulose to glucose. ACS Sustain. Chem. Eng. 7, 3339–3348.
Xie, T., Liu, Z.C., Liu, Q., Wang, G.G., 2015. Structural insight into the oxidation of sinapic acid by CotA laccase. J. Struct. Biol. 190, 155–161.
Zhao, G., Wang, J., Li, Y., Chen, X., Liu, Y., 2011. Enzymes immobilized on superparamagnetic Fe_3O_4@clays nanocomposites: preparation, characterization, and a new strategy for the regeneration of supports. J. Phys. Chem. C 115, 6350–6359.
Zhu, Q.Q., Zhuang, W., Chen, Y., Wang, Z.K., Wu, B.V.J.L., Yang, P.P., Liu, D., Zhu, C.J., Ying, H.J., Zhu, Z.H., 2018. Nano-biocatalysts of cyt c@ZIF-8/GO composites with high recyclability via a de novo approach. ACS Appl. Mater. Interfaces 10, 16066–16076.